2-2015

An Unusual Aerial Photograph of an Eddy Circulation in Marine Stratocumulus Clouds (Picture of the Month)

Bradley M. Muller
Embry-Riddle Aeronautical University

Christopher G. Herbster
Embry-Riddle Aeronautical University

Frederick R. Mosher
Embry-Riddle Aeronautical University, moshe774@erau.edu

Scholarly Commons Citation

Muller, B. M., Herbster, C. G., & Mosher, F. R. (2015). An Unusual Aerial Photograph of an Eddy Circulation in Marine Stratocumulus Clouds (Picture of the Month). *Monthly Weather Review, 143*(2). https://doi.org/10.1175/MWR-D-13-00316.1

PICTURE OF THE MONTH

An Unusual Aerial Photograph of an Eddy Circulation in Marine Stratocumulus Clouds

BRADLEY M. MULLER, CHRISTOPHER G. HERBSTER, AND FREDERICK R. MOSHER

Department of Applied Aviation Sciences, Embry–Riddle Aeronautical University, Daytona Beach, Florida

(Manuscript received 5 October 2013, in final form 16 October 2014)

ABSTRACT

An aerial photograph of a cyclonic, von Kármán–like vortex in the marine stratocumulus clouds off the California coast, taken by a commercial pilot near Grover Beach, is presented. It is believed that this is the first photograph of such an eddy, taken from an airplane, to appear in publication.

The eddy occurred with a strong inversion above a shallow marine boundary layer, in the lee of high, inversion-penetrating terrain. Tower and surface wind measurements plotted on satellite imagery demonstrate that the Grover Beach eddy was not just a cloud-level feature, but extended through the marine atmospheric boundary layer (MABL) to the surface. Evolution of the flow during the formation of the eddy appears similar to idealized numerical simulations of blocked MABL flow from the literature. The tower measurements sampled the northern part of the eddy circulation during its formation just offshore. The 2°–3°C temperature increases and then decreases during and after the eddy passage may be indicative of warmer air, from sheltered locations to the southeast, and/or downslope flow, being advected by and included into the eddy circulation. Satellite data compared with sequences of wind reversals at two different levels of the meteorological tower suggest that the eddy is tilted with height, at least during its formation stage. Formation mechanisms are discussed, but the subsynoptic observations are inadequate to resolve basic questions about the flow; ultimately a high-resolution model simulation is needed.

1. Introduction

On 12 September 2006, a pilot flying California coastal routes for SkyWest Airlines observed and photographed a cyclonic vortex in marine stratocumulus clouds just off the coast (Capt. P. Weiss 2006, personal communication). It was spotted off Grover Beach downwind of a coastal headland (Fig. 1) southwest of San Luis Obispo, California, within a generally northwesterly marine atmospheric boundary layer (MABL) flow regime. Based on estimates from the Geostationary Operational Environmental Satellite (GOES) imagery, this eddy circulation in the clouds appeared to be on the order of 10–20 km in diameter, placing it on the borderline between the meso-gamma and meso-beta scales of phenomena [2–20 and 20–200 km, respectively; Orlanski (1975)]. It contained a round cloud-free "eye" or hole of 2–3-km diameter at its center.

Casual inspection of GOES imagery of the West Coast region of North America reveals that similar eddies in the stratocumulus-topped MABL, on the order of tens of kilometers, are a relatively common occurrence near peninsulas, headlands, and downwind of islands. Many investigators have likened these relatively small-scale circulations, and similar features in other parts of the world, to von Kármán vortices (Hubert and Krueger 1962; Chopra and Hubert 1965; Lyons and Fujita 1968; Thomson et al. 1977; Ruscher and Deardorff 1982; Etling 1989; Young and Zawislak 2006).

A number of meso-beta-scale (20–200 km) eddies appear on a regular basis in the nearshore marine environment and have been described in the literature. They include the Catalina eddy (e.g., Rosenthal 1968; Bosart 1983; Wakimoto 1987; Mass and Albright 1989; Eddington et al.1992; Thompson et al. 1997; Parish et al. 2013), the Gaviota and midchannel eddies (Kessler and Douglas 1991; Douglas and Kessler 1991; Hanna et al. 1991; Wilczak et al. 1991;

Denotes Open Access content.

Corresponding author address: Dr. Bradley M. Muller, Dept. of Applied Aviation Sciences, Embry-Riddle Aeronautical University, 600 S. Clyde Morris Blvd., Daytona Beach, FL 32114-3900.
E-mail: mullerb@erau.edu

DOI: 10.1175/MWR-D-13-00316.1

FIG. 1. Aerial photograph of stratocumulus cloud vortex just offshore from Grover Beach, CA, at 1128 PDT (1828 UTC) 12 Sep 2006. (Photo by "KB" courtesy of Capt. P. Weiss of SkyWest Airlines.)

Dorman and Winant 2000), the Santa Cruz eddy (Archer et al. 2005; Archer and Jacobson 2005), and the Antalya cyclone (Alpert et al. 1999). Eddies at this scale are important because they are persistent and large enough to influence local stratus cloud formation, air quality, and surface wind fields in coastal regions (Wakimoto 1987; Hanna et al. 1991; Archer et al. 2005). The preceding modeling and observational studies indicate that these eddies result from complex interactions between a strong boundary layer–topping marine inversion, inversion-penetrating terrain, synoptic-scale wind and pressure fields, nighttime drainage flows, and daytime/nighttime wind reversals produced by diurnal radiative cycles.

The smaller borderline meso-gamma/meso-beta-scale eddy photographed and investigated in the current research appears to be a mechanically driven transient feature [see the discussion by Hubert and Krueger (1962)], lasting several hours. Such order-10-km eddies are important as they have been hypothesized to play a role in mixing at the coastal margin and have been implicated in cross-inversion fluxes of ozone and momentum (Lester 1985). Furthermore, they could lead to unexpected wind shifts for sailors or pilots, and anecdotal reports suggest an environment of strong aircraft turbulence in the lee of islands that produce similar eddies (B. Baxter and P. Ruscher 2012, personal communication). Indeed, strong turbulence in the lee of the Hawaiian island of Kauai was documented as a cause of the breakup and crash of the National Aeronautics and Space Administration's (NASA's) ultralight unmanned aerial vehicle, Helios (Porter et al. 2007). While the satellite imagery indicates that its appearance and scale are similar to those found in Von Kármán vortex streets (e.g., Young and Zawislak 2006), the eddy presented here occurred individually and not as part of a series, although evidence will be presented that the Grover Beach eddy actually was the second one to form in the area that morning.

While radiometric imagery of such features from weather satellites is common, the case presented in this paper is notable in that *photographic* documentation of atmospheric eddies at this scale has been lacking in the meteorological literature. To our knowledge, this is the first close-up photograph of a marine stratocumulus eddy, taken from an airplane, to appear in publication. Furthermore, because of their small scale, similar eddies often pass between observation stations or occur within island wakes over the open ocean making them difficult to measure directly. This has left some basic questions not completely resolved, such as the nature of the cloud-free eye, and whether their circulations are only an inversion-level feature (as indicated by their cloud-free eye) or if they penetrate through the MABL all the way to the surface (Young and Zawislak 2006).

Given the relative frequency of mechanical eddies in satellite imagery, we have concluded that pilots on the

U.S. West Coast must see them periodically, but the current example seems to be one of the few times that an actual photograph has come to light in a scientific context. Our speculations were anecdotally corroborated by a colleague who remembers seeing them frequently while flying routes between Monterey and El Toro, California, for the U.S. Marine Corps (F. Richey 2013, personal communication).

The purpose of this paper is to present this unusual photographic image of an eddy near Grover Beach, to document its formation and physical characteristics to the extent possible given the limited data available, and to discuss hypotheses from the theoretical literature pertinent to its formation. It is intended that information about the Grover Beach eddy will serve as a benchmark for verification and corroboration of numerical model simulations and studies on predictability of small-scale coastal effects. This paper demonstrates the value, but also the limitations of existing high-resolution coastal monitoring sites for detailed understanding of coastal processes. Confirmation of the photographed cloud feature is provided in the form of corresponding satellite imagery, allowing nearly the complete eddy life cycle to be examined over a time span of approximately five hours. Soundings, surface, and tower data will demonstrate that the circulation occurred with a very strong temperature inversion above a relatively shallow MABL, and was present at the surface as well as cloud level. Additionally, evidence of the inclusion of locally modified air in the eddy circulation will be presented in the form of time series of winds and temperature as the Grover Beach eddy formed near the Pacific Gas and Electric Company (PG&E) instrument tower. The paper is organized as follows. Meteorological data sources are detailed in section 2a. The synoptic meteorological setup will be described in section 2b, and a detailed description and analysis of the eddy are presented in section 2c including a brief comparison of the evolution of the observed flow field with that described in relevant modeling scenarios. Nondimensional control parameters for eddy formation are described and estimated in section 2d. Values for the control parameters will be discussed in the context of the theoretical literature on eddy formation in section 2e. Section 3 presents the summary and conclusions.

2. Satellite imagery and meteorological environment of the Grover Beach eddy

a. Special meteorological data sources and eddy overview

Three subsynoptic data sources provide information about the Grover Beach eddy. Locations of the most relevant stations from these sources in relation to the terrain that produced the eddy are shown in Fig. 2. Directly north-northwest of San Luis Bay is a headland containing the San Luis Range (also known locally as the Irish Hills) with the higher ridges extending to between 450 and 550 m (1500–1800 ft) MSL. The Los Osos Valley and San Luis Obispo can be found to the northeast. Pt. Buchon, the westernmost location on the headland is to the northwest of San Luis Bay while Grover Beach is to the south southeast. Much of the terrain all along the southwest flank of this steep headland formed by the San Luis Range rises to more than 300 m (1000 ft) MSL of elevation within a kilometer of the coastline.

The first special data source is a three-station network operated by PG&E in support of their Diablo Canyon nuclear power plant (Thuillier 1987). These stations consist of a 10-m tower located at Pt. Buchon at an elevation of 12.2 m (40 ft), a 20-m tower on Davis Peak in the San Luis Range at an elevation of 549 m (1800 ft), and their ''primary meteorological'' site, a 76-m tower at the plant itself (hereafter referred to as the ''meteorological tower'') at 32 m (105 ft) MSL. The tower measures winds at 10 and 76 m AGL, and temperature at 10, 46, and 76 m AGL. Pressure and humidity are not measured. Data from these stations were available every 15 min. The second data source is from the meteorological station at the California Polytechnic State University (Cal Poly) Center for Coastal Marine Sciences Pier in San Luis Bay. This station contains a full suite of meteorological measurements on a 4-m tower, archiving data every 2 min. The third dataset comes from wind-monitoring instruments operated by the San Luis Obispo County Air Pollution Control District (SLOAPCD), collecting observations every minute.

It should be noted that at the scales being examined in this paper, distances of less than a few kilometers and time periods of a few minutes become important for matching wind observations to satellite features. For example, at a speed of 3 m s^{-1} the eddy can move nearly 2.7 km, roughly the diameter of the cloud-free eye when photographed, in 15 min. Therefore, special care was taken to match images as closely as possible with the appropriate observation time. This involved calculating the time for the GOES-West imager radiometer to scan to the latitude of the Diablo Canyon area, then determining the closest observations to that time for each of the three data sources: the 15-min PG&E data, the 2-min Cal Poly data, and the 1-min SLOAPCD data. There can be a 1–4-min lag time between the beginning of the GOES-West scan and the time it takes to reach the latitude of the Diablo Canyon area, depending on which sector it is scanning. Additionally there can be

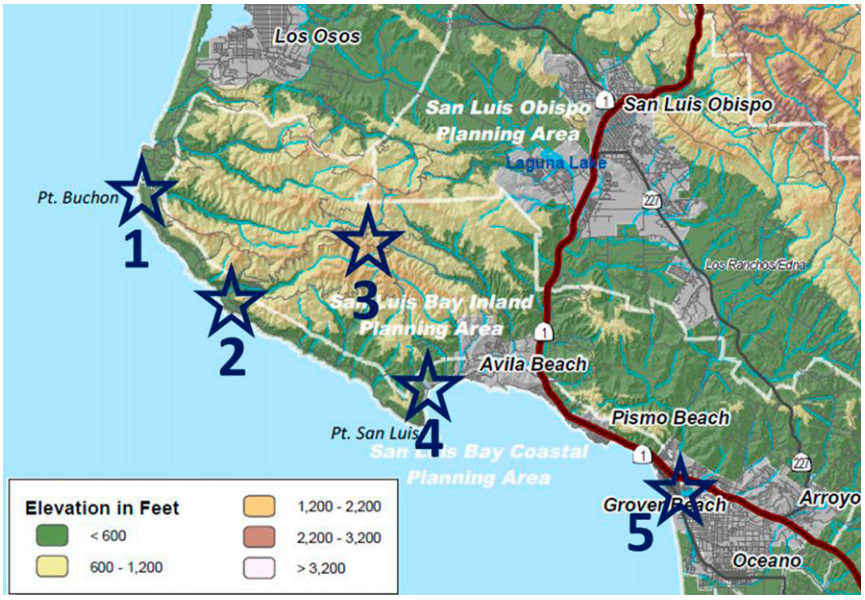

FIG. 2. Terrain that produced the Grover Beach eddy, with the locations of relevant monitoring stations superimposed and numbered as follows: 1) Pt. Buchon, 2) Diablo Canyon nuclear power plant meteorological tower, 3) Davis Peak, 4) Cal Poly pier, and 5) SLOAPCD Grover Beach site. Just to the north-northwest of San Luis Bay is the San Luis Range (also known locally as the Irish Hills), which has ridges extending to between 450 and 550 m (1500–1800 ft) MSL. (Base map courtesy of San Luis Obispo County Planning Department, Geographic Technology and Design Section.)

errors of 1–2 km in the satellite navigation. For these reasons there is some uncertainty in discerning exact locations of eddy formation and movement.

GOES observations with the subsynoptic data superimposed using Unidata's Integrated Data Viewer (IDV) are presented in Fig. 3. The satellite data were obtained from the National Oceanic and Atmospheric Administration (NOAA) Comprehensive Large Array-Data Stewardship System (CLASS), remapped to a local perspective using the Man Computer Interactive Data Access System (McIDAS), then displayed and analyzed using the Global Atmospheric Research Program (GARP) General Meteorology Package (GEMPAK) Analysis and Rendering Program. The images were brightness normalized (Mosher 2013) and contrast enhanced to better view early morning cloud features.

The eddy originally emerged offshore just south of Pt. Buchon. Subsequently it advected to the southeast with the mean northwesterly MABL flow, then turned toward the east. As it approached Grover Beach from the west it was photographed by the pilot at 1828 UTC (Fig. 1), finally making landfall at Grover Beach between 1830 and 1900 UTC, approximately 3–4 h after its inception.

b. *Synoptic conditions*

Synoptic-scale weather conditions at the surface and 850 hPa at 1200 UTC 12 September 2006 are shown in Fig. 4. The prevailing surface airflow over the ocean as reported by buoy stations is climatologically typical [i.e., northwesterly at around 5 m s^{-1} (10 kt)]. Several stations in the vicinity of the south-central California coast were reporting fog or mist. At 850 hPa there was a west–east-oriented ridge of high pressure north of the Grover Beach area resulting in offshore (easterly) flow above the boundary layer over the south-central California coast.

The marine layer in the central and Southern California coastal region was very shallow. For example, the 1200 UTC Oakland, California, sounding 320 km to the north-northwest (left panel, Fig. 5) indicated a surface-based temperature inversion. Profiler data from Fort Ord, 195 km to the north-northwest (not shown), also indicated a surface-based temperature inversion with northeasterly flow above the boundary layer. The San Diego, California, sounding 420 km to the southwest (right panel, Fig. 5) indicated an inversion base at 251 m. (It would be preferable to use the sounding from the much-closer Vandenberg raob site to characterize the environment of the Grover Beach eddy, but crucial data were missing from its lower levels.) Satellite imagery showing the intersection of stratocumulus clouds with terrain elevation (not shown) suggest that the MABL depth near the San Luis range was no more than 200 m prior to eddy formation. A presunrise temperature of 25°C with steady northeast winds at PG&E's Davis Peak

station at an elevation of 550 m (1800 ft) compared with 11.5°C at the 10-m meteorological tower level confirms that the San Luis range penetrated above the MABL into the inversion.

c. Grover Beach eddy description and analysis

According to the image properties received with the picture, the Grover Beach eddy was photographed at 1128 PDT (1828 UTC) looking toward the west-southwest (Fig. 1). Visible satellite imagery (Fig. 3) corroborates the existence of this flow feature and allows us to track the eddy's life cycle and estimate its dimensions. The 1830 UTC satellite image (11th panel in Fig. 3) is the time closest to the photograph time. Estimates made using GARP indicate that the eddy had a width of 9 km, was 17 km in length, and contained a cloud-free eye of 2.5–3 km at the time the photograph was taken. When first evident on the satellite imagery as it emerges near the coastline, the cloud-free eye is 6–7 km in diameter, but shrinks to 2–3 km as it turns from moving southwestward to moving toward the east. The shrinkage of the eye is similar to that of von Kármán vortices seen downwind of islands (Young and Zawislak 2006), suggesting a nonsteady-state boundary layer flow characterized by pressure gradient force, centrifugal force, and friction.

Satellite images at 1445, 1500, and 1530 UTC (Fig. 3) show a sharp boundary between clear and cloudy air, initially near the coastline, bulging toward the southwest over the ocean in line with the northeasterly winds *above* the MABL at Davis Peak, establishing the cloud-free eye feature by 1600 UTC. The sharpness of the boundary suggests the possibility of confluent airstreams at cloud level between the northeasterly winds aloft descending in the lee of the San Luis range and the northwesterly winds in the MABL, although there is no evidence of such winds at tower level during this time.

During its lifetime on satellite imagery, the eddy is close enough to influence surface wind measurements at three different observing stations (Fig. 3). Each encounter is consistent with cyclonic circulation. The associated wind shifts can be seen at the meteorological tower beginning at 1530 UTC, the Cal Poly pier at 1746 UTC, and the Grover Beach station starting around 1830 UTC. Notably, after being photographed just offshore by the pilot at 1830 UTC, the eddy moved inland directly over SLOAPCD's wind monitoring station, causing a nearly 180° wind direction reversal over a period of 1 min. These in situ wind measurements corroborate Li et al.'s (2000) synthetic aperature radar results and Heinze et al.'s (2012) large-eddy simulation (LES) results that the circulations of von Kármán vortices observed in satellite imagery of island wakes extend through the depth of the MABL to the surface.

It is interesting to note some features seen early in the eddy's life at 1600 UTC (Fig. 3): specifically, a band of clouds in the northwesterly flow piling up against the northwest face of the headland containing the San Luis Range, and a very similar band on the northwest flank of the cloud-free eye. Outside that is a dark band of apparently thin, less reflective clouds. These features are marginally reminiscent of "shock" phenomena (e.g., Jiang and Smith 2000; Burk and Thompson 2004), but are not clear cut and no real conclusions can be drawn. Near the eddy these dark and light bands form in the convergence between the northwesterly MABL seen at this time at Pt. Buchon and the oppositional southeasterly flow on the northern side of the eddy. The result is a rim of thick, bright clouds surrounded by a dark area of thin clouds that at subsequent times is advected by the eddy circulation, encircling and spiraling inward toward the eye over time. The interweaved dark and light bands in the aerial photograph of the eddy (Fig. 1, corresponding to the 1830 UTC image in Fig. 3), of course, show considerably more detail than the satellite imagery, and it remains to be explained, perhaps by a very high-resolution model simulation, what the exact mechanisms are that produce the detailed structure.

Figure 6 shows two panels of a time series of winds and temperatures from PG&E's meteorology tower covering the periods 0900–1400 and 1400–1900 UTC 12 September 2006, with simultaneous winds and temperatures from the Cal Poly pier also included for reference. Based on the satellite imagery (Fig. 3), the Grover Beach eddy formation and passage near the meteorological tower occurs approximately between 1445 and 1645 UTC. The 1415–1445 UTC images show the apparent remnants of a previous eddy affecting the winds at the Cal Poly pier. The top panel in Fig. 6 showing time series of the meteorology tower between 0900 and 1400 UTC is included because it also contains an apparent previous eddy passage between approximately 1015 and 1215 UTC that may be the same one seen later (horseshoe-shaped dark area) in Fig. 3 at 1415 UTC near the Cal Poly Pier.

In terms of the prevailing northwesterly MABL flow in which the eddy occurred, Pt. Buchon is at the corner of the upwind face of the headland containing the San Luis Range, while the Cal Poly pier and the Grover Beach station are "downstream." Flow blocking has been highlighted as a key element of eddy formation (some relevant literature will be discussed in section 2e). Epifanio and Rotunno (2005) emphasize the role of blocking, so it is instructive to briefly review the evolution of their wake flow for comparison with the Grover Beach case. In their Fig. 10, fluid piles up on the upwind face of the obstacle, while on the downwind side there is a deficit,

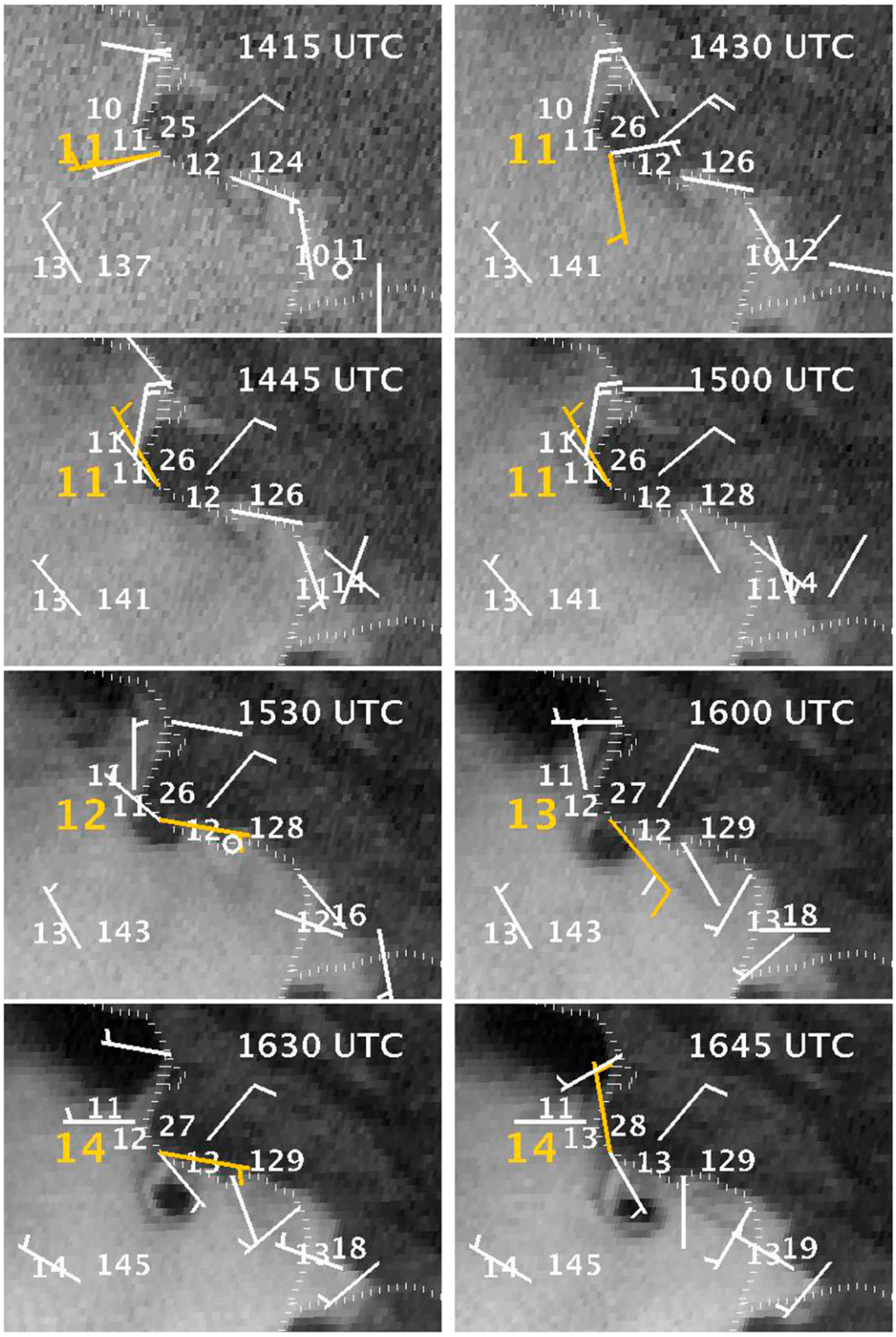

FIG. 3. GOES-West images from 1415 to 1911 UTC 12 Sep 2006 showing the Grover Beach eddy. The satellite image at 1830 UTC shows the same cloud as in Fig. 2. Analysis of the image shows a length of 17 km, a width of 9 km, and a cloud-free eye of 2.5–3 km. Half-barbs represent wind speeds of approximately 2.5 m s^{-1}. Whole barbs represent wind speeds of approximately 5 m s^{-1}, and a shaft with no barb represents wind speeds of less than approximately 1.3 m s^{-1} but greater than 0.26 m s^{-1}. Circles depict wind speeds of less than approximately 0.26 m s^{-1}. Temperatures are in °C. The meteorological tower 76-m level temperatures and winds are plotted in orange with larger symbols on top of the 10-m temperatures and winds.

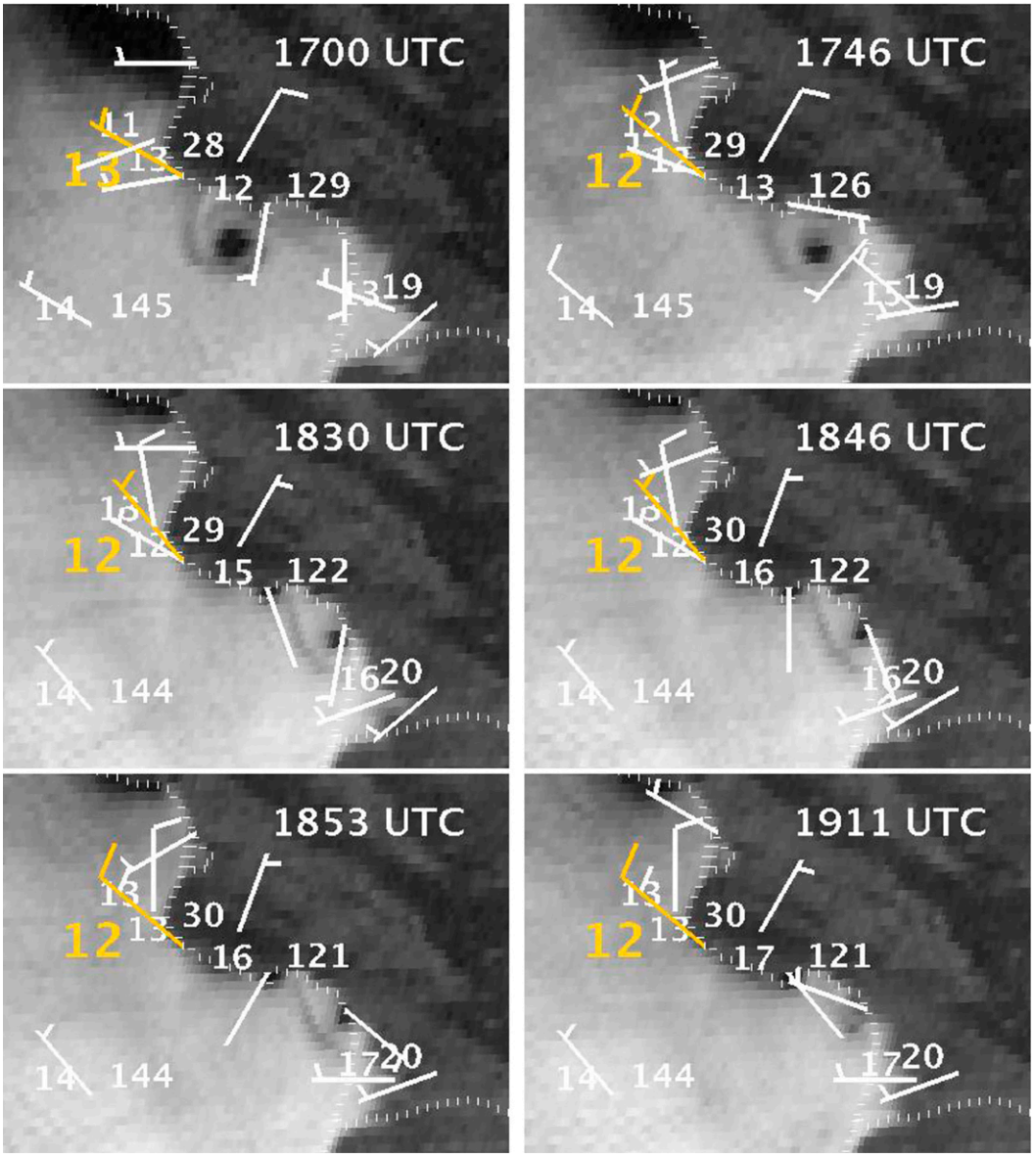

FIG. 3. (*Continued*)

especially at the two lateral edges of the terrain. Gravity forces fluid in the lee to flow back toward the obstacle into the deficit, forming a wake region of reversed flow (i.e., moving opposite to the undisturbed upstream flow), and "tentacles" of vorticity extend downstream along shear lines bounding the wake. Ultimately this return flow curls around regions of fluid deficit on both lateral edges of the terrain forming counter-rotating eddies with inclusions of warm air at their cores. Qualitatively similar results can also be seen in Fig. 1 in Smolarkiewicz and Rotunno (1989a, hereafter SR89a), Fig. 1 in Smolarkiewicz and Rotunno (1989b), and Fig. 7 in Schär and Smith (1993, hereafter SS93).

In the current case, from 1415 to 1500 UTC, just prior to eddy formation, the satellite images and surface data (Fig. 3) indicate that some of the prevailing northwesterly MABL flow is temporarily being blocked and forced to deviate to its right (looking downstream) around the headland as seen in the northerly winds of approximately 7.5 m s^{-1} rounding Pt. Buchon. There is considerable horizontal cyclonic shear between the winds of Pt. Buchon and those at the meteorological tower, which most likely contributes to the eventual formation of the eddy. Additionally, reversed boundary layer flow is seen at the Cal Poly pier and Grover Beach in the form of southeasterly winds blowing back toward

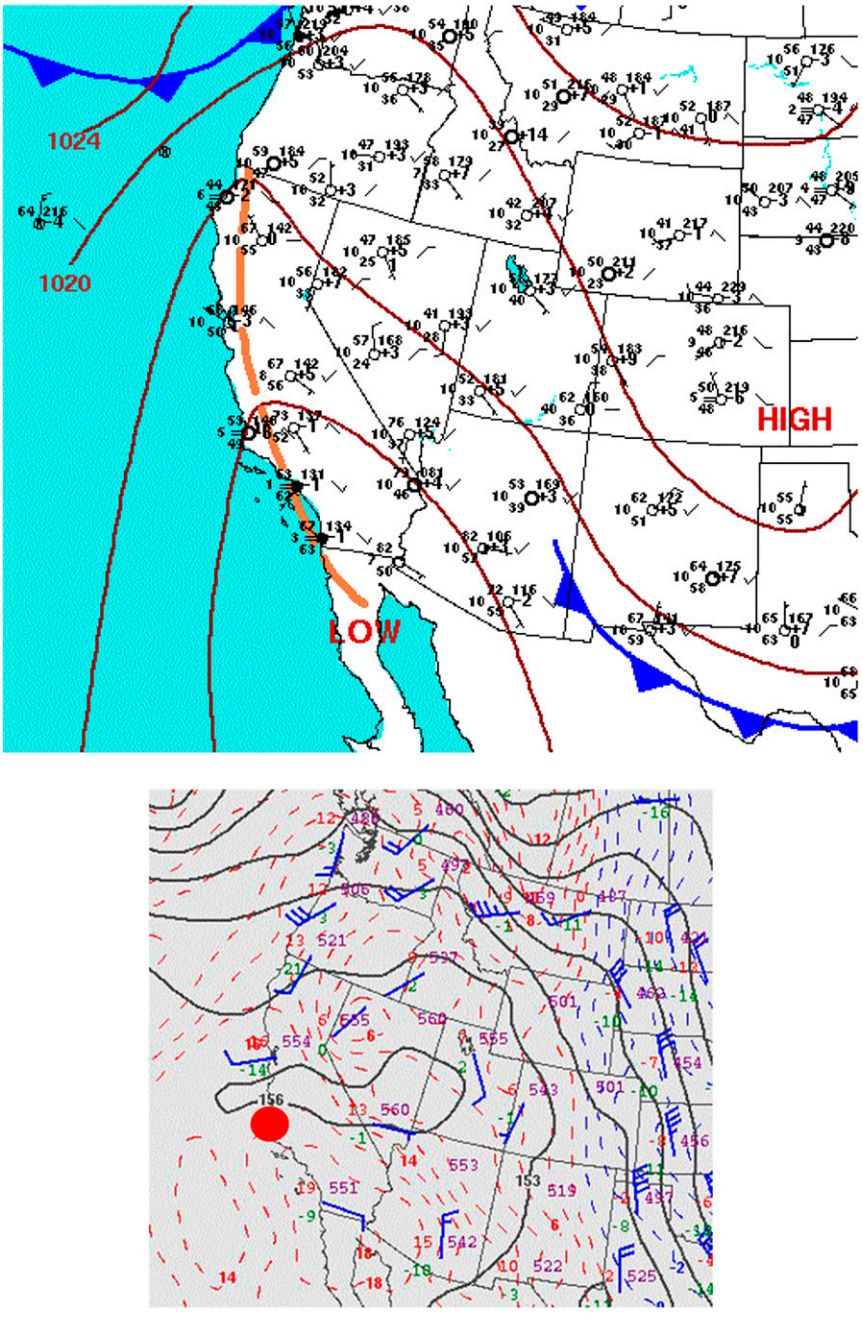

FIG. 4. (top) Surface analysis for 1200 UTC 12 Sep 2006 from the Weather Prediction Center's Daily Weather Maps archive. (bottom) The 850-hPa chart for 1200 UTC 12 Sep 2006 from the Storm Prediction Center archive. The 850-hPa winds from the Oakland and San Diego soundings can be seen along the central and southern California coast. Heights are in decameters and winds are in knots. The red dot shows the location of the Grover Beach eddy.

the San Luis Range. An apparent (dark) shear line between the northwesterly winds at the meteorological tower and the southeasterly winds at the Cal Poly pier can be detected west of Pt. San Luis in the GOES-West imagery at 1445 UTC. By 1500 UTC, a strand of clouds begins to move northwestward along the coast toward the meteorological tower, while simultaneously the boundary of cloud-free air is pushing southwestward perpendicular to the coastline, in line with the northeasterly winds aloft at Davis Peak. By 1530 UTC the tongue of clouds has nearly reached the meteorological tower and winds at the 76-m level shift from northwesterly

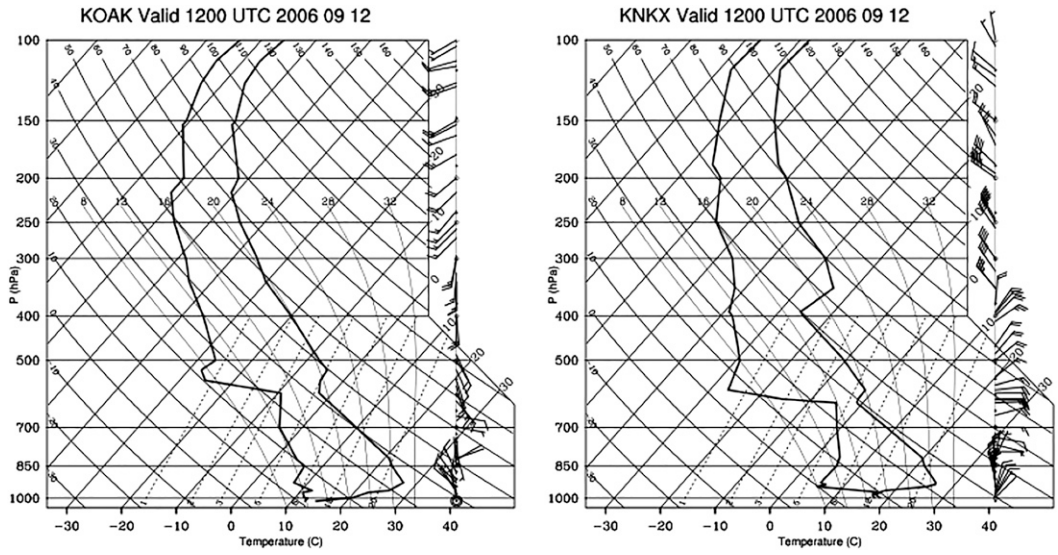

FIG. 5. (left) Oakland (KOAK) sounding at 1200 UTC 12 Sep 2006. (right) San Diego (KNKX) sounding for the same time.

to southeasterly, while the 10-m winds are still northwesterly. At 1600 UTC the clouds appear to completely encircle the cloud-free air of the eye.

It is interesting to note that the wind shift to southeasterly at 76 m seen in the 1530 UTC panel in Fig. 3 precedes that at the 10-m level, which is still northwesterly, by 15 min (see Fig. 6). In general, the 76-m winds seem to respond sooner and with more apparent synchronicity to features in the satellite imagery than do the winds at the 10-m level. This is seen again from 1630 to 1700 UTC where the changes in wind direction at 10 m seem to lag those at 76 m, and both levels lag the apparent eddy position at cloud top as indicated by the satellite features. The better agreement between cloud features and the 76-m level winds conceivably is owing to their position nearer to cloud level, and suggests the possibility of the eddy tilting with height. One can imagine the surface levels of the eddy ''dragging behind'' due to the greater restraining effect of surface friction on the advection of the eddy at 10 m than at 76 m or cloud level. Dorman and Koračin (2008) refer to this effect on MABL flow in general by citing aircraft soundings showing that surface-level buoy winds underestimate the layer wind speed. Thus, they multiplied buoy winds by a factor of 1.15 to estimate representative wind speeds of the MABL for the calculation of Froude numbers.

A downstream tilt with height was seen in the mesoscale model simulations of island wake vortices of Sun and Chern (1994). On the other hand, Heinze et al. (2012) simulated vortex streets using an LES model, and noted that the eddies were oriented vertically, even with a no-slip condition at the lower boundary. This was attributed to a well-mixed vertical profile of velocity in the MABL. However, they were sampling the simulated eddies *after* the formation process, whereas the tower data are sampling only the northern part of the circulation during its formation/organization process. It is possible that boundary layer mixing processes establish a more vertically oriented eddy *after* formation, since our eddy shows very close synchronicity between the cyclonic wind shift at Grover Beach and the cloud-free eye passage in satellite imagery (see Fig. 3 for 1846, 1853, and 1911 UTC).

In general, local temperatures in coastal California during the summer are strongly modulated by their exposure to the MABL based on the local terrain. Protected locations typically have a considerably warmer microclimate during the daytime than places that receive the direct influence of the MABL. The temperature curves in Fig. 6 (bottom panel) show that just prior to the eddy formation (i.e., before about 1500 UTC) the entire 76-m tower was within the well-mixed MABL. Temperatures were close to 11°C for all three tower levels. Temperatures at the Cal Poly pier to the southeast are nearly 1°C warmer than those at 10 m. Temperatures at 76 m climb out of the well-mixed regime at 1530 UTC with the onset of easterly winds at that level, establishing a surface-based temperature inversion. It is not possible to determine from the data whether this new inversion is related to the large-scale subsidence inversion already present at higher levels, or is just a consequence of local differential advection and/or downslope motion off the higher terrain. The greatest

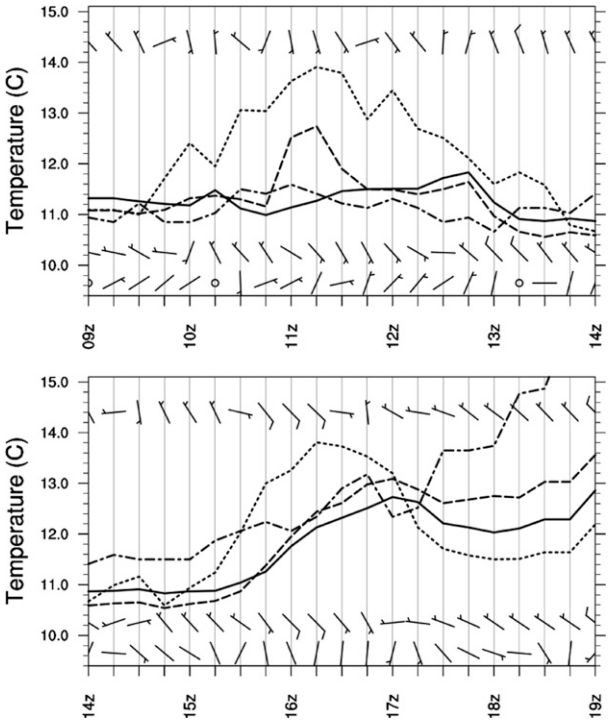

FIG. 6. Temperature (°C) time series (curves) from three tower levels and the Cal Poly pier, and wind time series (barbs) from two levels collected by the instrumented tower at the Diablo Canyon nuclear power plant, and the Cal Poly pier. The dotted curve is from 76 m, the dashed curve is from 46 m, the solid curve is from 10 m above ground level (AGL) at the tower, while the dash–dot curve is from the Cal Poly pier. The top row of winds is from 76 m, the second row is from 10 m AGL, and the bottom row is from the Cal Poly pier. Half barbs indicate approximately 2.5 m s^{-1} and whole barbs approximately 5 m s^{-1}. Time is in UTC. Based on satellite imagery, the eddy passage at the tower is roughly between 1445 and 1615 UTC. Vertical lines mark the times of the tower observations. Note that the fastest winds and the warmest temperature at 76 m during the period occur in the southeasterly flow of the eddy's northern flank. A previous eddy with a similar magnitude warming at 76 and 46 m occurred near the tower roughly between 1015 and 1215 UTC.

rate of temperature increase at all tower levels occurs within the "return flow" southeasterly winds on the northeast and north side of the cloud-free eye, with temperature peaking at 14°C at 1615 UTC at 76 m *after* the eye has already moved to the south. At 10 m the peak temperature is even later, occurring at 1700 UTC, clearly outside the eddy's apparent circulation based on satellite imagery.

While warm cores are predicted for wake vortices (SR89a; Schär and Durran 1997), lack of synchronicity between the warming temperatures and the apparent eddy location in the satellite imagery suggests advection of warmer air from the more protected locations to the southeast, possibly as part of the wake return flow that helped to generate the eddy. Surface temperatures from the Cal Poly pier to the southeast (Fig. 6) suggest that the warmer air from that area can account for the 10-m temperature changes at the tower with the onset of the southeasterly winds. Once the northwest winds are reestablished, tower values are decoupled from temperatures at the pier, which continue to climb under the influence of surface heating, diverging from those at the tower. While the tower temperatures at first drop with the northwesterly winds, they do not settle back to their original pre-eddy values, probably due to the influence of solar heating.

The first panel in Fig. 6 was included because it also appears to contain eddy warming, but with the solar heating signal removed (sunrise is at 1345 UTC). Cal Poly pier temperatures are cooler than those at the 10-m tower, and therefore southeasterly winds at that level do not bring the magnitude of warming seen in the second panel. At 76 m, temperature rises again seem to be predominantly linked with southeasterly flow, while falling temperatures correlate with northwest winds. This case corroborates the idea that the warming is most likely advective and possibly downslope. Available sources of warm air include the more protected area to the southeast, the synoptic-scale temperature inversion, or even air from above a nighttime radiation inversion. A final point is that while it is tempting to infer the warming as part of the dynamics of warm core eddy formation, the LES simulations by Heinze et al. (2012) show warm anomalies in the center of wake vortices of only about 0.3 K. The tower apparently did not sample the center of the eddy, and unfortunately there was no temperature sensor on the Grover Beach station, so we do not know how temperature anomalies in the core of the eddy compare to the LES model simulation.

d. *Shallow-water Froude number, nondimensional mountain height, and blocking effects*

Many investigators have employed a "shallow water" Froude number to characterize the MABL along the California coast in analogy to hydraulic theory (Rahn et al. 2013; Dorman and Koračin 2008; Archer and Jacobson 2005; Burk and Thompson 2004; Haack et al. 2001, to name a few). The upstream shallow-water Froude number Fr_∞ can be written as

$$\mathrm{Fr}_\infty = \frac{U_{\mathrm{MABL}}}{\sqrt{g\left(\frac{\theta_t - \theta}{\theta}\right)H}}, \tag{1}$$

where U_{MABL} is the undisturbed wind speed in the MABL upwind of the eddy-producing terrain, g is the acceleration of gravity, H is the upwind depth of the

MABL, θ_t is the potential temperature at the top of the inversion, and θ is the potential temperature of the MABL. In the shallow-water framework, a nondimensional mountain height,

$$M = \frac{h_m}{H}, \tag{2}$$

is needed in addition to the Fr_∞ to discriminate flow-over versus flow-around regimes (SS93), where h_m is the height of the terrain that produced the eddy, taken as 550 m. The fluid (in our case the MABL flow) is blocked if $M > M_s$, where

$$M_s = 1 + \frac{1}{2}Fr_\infty^2 \tag{3}$$

is a form of the Bernoulli equation (SS93). SS93 delineate a parameter-space of M versus Fr_∞ that is useful for the current study. Values of M_s delineate the boundary between their "regime II," where $M < M_s$ and fluid can flow over an obstacle, and "regime III" where $M > M_s$, and fluid is blocked by the obstacle and flows around it.

Since the Vandenberg sounding was missing crucial data, our approach for calculating Fr_∞ and M employs local and upstream bracketing values of the input variables to estimate constraining ranges of these control parameters. Potential temperature quantities were obtained from the meteorological tower and Davis Peak. Winds from buoy 46028, 105 km northwest of Pt. Buchon, were used to subjectively determine a constraining range of upstream wind speeds, U, and a 24-h average value. Following the procedure of Dorman and Koračin (2008), these Us were multiplied by a factor of 1.15 to obtain the U_{MABL} values. Maximum and minimum values of H were estimated through recognition that (i) prior to eddy formation, the meteorology tower was completely within the MABL, so the undisturbed depth must be no less than 108 m (i.e., 76 + 32 m of elevation) and (ii) satellite-based clouds overlaid on terrain intersected at a maximum elevation of 200 m. Results based on the preceding estimates are given in Table 1 and are discussed in the next section.

e. Discussion

Dorman and Koračin (2008) define transcritical flow as Fr_∞ values between 0.5 and 1.0, which is expected to become locally supercritical (i.e., Fr > 1) under the influence of the coastline terrain, potentially leading to hydraulic features in the MABL such as expansion fans and hydraulic jumps (Jiang and Smith 2000). This is important, because wake vortex simulations of blocked flow highlight hydraulic jumps (sometimes also described as "shock" features) as a key element of vorticity and potential vorticity (PV) production. Our Fr_∞ results for the more probable upstream wind speeds of 5 and 6 m s^{-1} range from 0.5 to 0.8 (Table 1); the less probable minimum U of 3 m s^{-1} gave values in the 0.3–0.4 range. Thus, the undisturbed boundary layer most likely met Dorman and Koračin's (2008) definition of transcritical flow. Furthermore, our bracketing values on M from Table 1 are 2.8 and 5.1, both greater than M_s, showing that the current case is within SS93's regime III of blocked flow. While it may seem an obvious and trivial result that the MABL cannot flow over the high terrain of the San Luis Range, more importantly, this allows us to select which of SS93's simulations is most comparable to our real-life case, and provides guidance for determining relevance out of a vast number of model realizations that can be found in the literature.

TABLE 1. Upstream Froude number Fr_∞ estimates from Eq. (1), nondimensional mountain height M from Eq. (2), and limiting value M_s for flow-over vs flow-around regimes from Eq. (3), where U represents approximate maximum, minimum, and mean wind values determined from buoy 46028 (105 km northwest of Pt. Buchon). These values are multiplied by 1.15 to obtain U_{MABL}. The H represents constraining values for the upstream depth of the MABL prior to eddy formation, θ was determined from the average of the 10- and 76-m tower values at 1400 UTC, while θ_t was determined from the simultaneous temperature value at Davis Peak. 1400 UTC is just prior to eddy formation when the entire tower was within the MABL. The MABL flow is blocked for $M > M_s$.

	H (max) = 200 m			H (min) = 108 m		
	Fr_∞	M	M_s	Fr_∞	M	M_s
U (max) = 6 m s^{-1}	0.6	2.8	1.2	0.8	5.1	1.3
U (mean) = 5 m s^{-1}	0.5	2.8	1.1	0.7	5.1	1.2
U (min) = 3 m s^{-1}	0.3	2.8	1.05	0.4	5.1	1.1

Early investigators of island wake vortices viewed eddy formation as an atmospheric process of lateral boundary layer separation. Through inviscid, uniformly stratified simulations, SR89a contributed the important ideas that lee eddies can form in the absence of friction so they do not require boundary layer separation, and that the source of vertical vorticity for the eddies is tilting of baroclinically generated vorticity due to sloping isentropes. SS93 confirm eddy formation in the absence of surface friction using a shallow-water model. They explain the eddies in terms of production of vorticity and PV by dissipation in a hydraulic jump. The Bernoulli function is used as a streamfunction of the total (i.e., advective plus dissipative) vorticity flux. Thus, gradients of Bernoulli function (which are especially pronounced in shock features) can be used to diagnose net vorticity flux (SS93). Schär and Durran (1997) extend ideas about Bernoulli gradients and PV generation to uniformly stratified flow. However, Epifanio and

Durran (2002a,b) point out that those studies do not offer a conceptual model to understand the vorticity and PV formation mechanisms. Their results corroborate the baroclinic generation and tilting mechanism of vertical vorticity proposed by SR89a, but they also quantitatively and conceptually make the physical connection that the vorticity is strongly amplified through stretching by hydraulic jump features that form on the lateral ends of the terrain, similar to those of SS93.

The basic evolution of wake flow in the blocked case was summarized from Epifanio and Rotunno (2005) in our section 2c. For the Grover Beach eddy, blocking parameters facilitate comparison to the shallow-water simulations of SS93, especially since simulations with a single layer of variable fluid depth seem to work well as analogs to a MABL capped by a strong temperature inversion as in the current case. Our constraining values of Fr_∞ and M (Table 1) are most like their simulation with $Fr_\infty = 0.5$ and $M = 2$, i.e., their flow-around regime III, which shows vorticity production at the terrain edges through the development of ''flank shocks'' (SS93's Fig. 7; Jiang and Smith 2000). And according to Epifanio and Durran (2002 a,b), eddy spinup would be aided by vertical stretching in the shocks. It should be noted that in our study there is no clear-cut evidence of flank shocks or jumps, so applicability of all these theoretical results remains uncertain.

The present case also is different than the modeling studies in that it is characterized by significant vertical shear in the wind field, with northwesterly winds in the MABL, but steady northeasterly winds in the inversion above the MABL, as seen at Davis Peak (Fig. 3). Vertical shear of this nature has not been studied in the idealized simulations cited above. Vertical shear is a source of horizontal vorticity. Tilting of shear-related horizontal vorticity to a vertical axis due to differential vertical motion could reinforce or counteract other vertical vorticity production mechanisms, depending on the details of the shear and vertical motion fields. Since observational data in the present case are not adequate to characterize these fields, we refrain from speculation, and will attempt to address this question in future research using numerical model simulations.

Casual examination of visible satellite images in the years since we received the eddy photograph has revealed that it is not uncommon for eddies to come spinning off the raised terrain of the San Luis Range. Its prominence as terrain that protrudes westward into the marine environment, while frequently penetrating the inversion above, creates conditions that are likely to produce eddies in ways similar to large islands like Santa Cruz and Catalina. The presence of the Diablo Canyon nuclear power plant and potential for toxic releases suggest that model simulations not only are necessary to better understand eddy formation mechanisms, but also would be useful to better characterize the complex flow characteristics in this region.

3. Summary and conclusions

A unique aerial photograph of a cyclonic eddy in the marine stratocumulus clouds, taken by a commercial pilot off the California coast, has been presented. The eddy was similar in scale and appearance to Von Kármán vortices seen in high-resolution satellite imagery and described in the literature. It had a cloud-free eye, and occurred under strong inversion conditions with a shallow MABL in the lee of inversion-penetrating terrain. To our knowledge, this is the first photographic image of such a feature, taken from an airplane, to appear in publication.

The Grover Beach eddy appeared from satellite imagery to form over the ocean near the three-level 76-m instrumented tower run by PG&E for monitoring at their Diablo Canyon nuclear power plant. Winds and temperatures on the tower responded to the eddy's circulation, as did winds at the Cal Poly pier, and Grover Beach. Winds at 76 m showed more synchronicity with satellite-observed eddy features than the winds at 10 m. The winds at 10 m showed similar responses but lagged those at 76 m by 15 min, suggesting that the eddy was tilting with height, at least at its inception. Both Fr_∞ and M calculations suggest that the MABL was most likely transcritical prior to eddy formation, and, therefore, hydraulic features such as hydraulic jumps were possible, although there was no unambiguous evidence of such phenomena. Calculated values of M and F_∞ indicate blocked flow, and therefore evolution of observed flow features appears qualitatively similar to eddy simulations involving blocked flow. Ultimately a high-resolution model simulation will be needed to answer questions about the relevance of eddy formation mechanisms described in the theoretical literature, and to determine the relative roles of both horizontal and vertical shear. Such simulations are under development in our laboratory.

Acknowledgments. This research became possible thanks to former Embry–Riddle Aeronautical University (ERAU) student and flight instructor, and current SkyWest pilot, Captain Peter Weiss, who originally sent us this unique eddy photograph, and ''KB'' who actually photographed the eddy. We gratefully acknowledge John Lindsey and Ed McCarthy of PG&E, Brian Zelenke of Cal Poly, and Gary Arcemont and Joel Craig of San Luis Obispo County Air Pollution Control District.

All were instrumental in providing the available meteorological observations. The base map used in Fig. 2 was obtained courtesy of the San Luis Obispo County Planning Department, Geographic Technology and Design Section. Pete Lester shared some difficult-to-find NSF reports. ERAU Applied Meteorology system administrator Robert Haley gave us invaluable assistance in data processing and with some of the figures. We thank Paul Ruscher, Bob Baxter, and Frank Richey for sharing their personal knowledge and experiences. The assistance of Dr. Mike Hickey and ERAU in providing funding for publication is gratefully acknowledged. We thank two anonymous reviewers whose comments significantly improved the manuscript.

This research benefited from several government-sponsored programs and software packages: NOAA's CLASS (http://www.class.ncdc.noaa.gov/saa/products/welcome); the McIDAS, GARP, and IDV software packages provided by NSF's Unidata program (http://www.unidata.ucar.edu/software/); and the National Center for Atmospheric Research (NCAR) Command Language (NCL) provided by NSF's NCAR (2014).

REFERENCES

Alpert, T., M. Tzidulko, and D. Iziksohn, 1999: A shallow, short-lived meso-β cyclone over the Gulf of Antalya, eastern Mediterranean. *Tellus,* **51A,** 249–262, doi:10.1034/j.1600-0870.1999.t01-2-00006.x.

Archer, C. L., and M. Z. Jacobson, 2005: The Santa Cruz Eddy. Part II: Mechanisms of formation. *Mon. Wea. Rev.,* **133,** 2387–2405, doi:10.1175/MWR2979.1.

——, ——, and F. L. Ludwig, 2005: The Santa Cruz Eddy. Part I: Observations and statistics. *Mon. Wea. Rev.,* **133,** 767–782, doi:10.1175/MWR2885.1.

Bosart, L. F., 1983: Analysis of a California Catalina eddy event. *Mon. Wea. Rev.,* **111,** 1619–1633, doi:10.1175/1520-0493(1983)111<1619:AOACCE>2.0.CO;2.

Burk, S. D., and W. T. Thompson, 2004: Mesoscale eddy formation and shock features associated with a coastally trapped disturbance. *Mon. Wea. Rev.,* **132,** 2204–2223, doi:10.1175/1520-0493(2004)132<2204:MEFASF>2.0.CO;2.

Chopra, K. P., and L. F. Hubert, 1965: Mesoscale eddies in wakes of islands. *J. Atmos. Sci.,* **22,** 652–657, doi:10.1175/1520-0469(1965)022<0652:MEIWOI>2.0.CO;2.

Dorman, C. E., and C. D. Winant, 2000: The structure and variability of the marine atmosphere around the Santa Barbara channel. *Mon. Wea. Rev.,* **128,** 261–282, doi:10.1175/1520-0493(2000)128<0261:TSAVOT>2.0.CO;2.

——, and D. Koračin, 2008: Response of the summer marine layer flow to an extreme California coastal bend. *Mon. Wea. Rev.,* **136,** 2894–2992, doi:10.1175/2007MWR2336.1.

Douglas, S. G., and R. C. Kessler, 1991: Analysis of mesoscale airflow patterns in the south-central coast air basin during the SCCCAMP 1985 intensive measurement periods. *J. Appl. Meteor.,* **30,** 607–631, doi:10.1175/1520-0450(1991)030<0607:AOMAPI>2.0.CO;2.

Eddington, L. W., J. J. O'Brien, and D. W. Stuart, 1992: Numerical simulation of topographically forced mesoscale variability in a well-mixed marine layer. *Mon. Wea. Rev.,* **120,** 2881–2896, doi:10.1175/1520-0493(1992)120<2881:NSOTFM>2.0.CO;2.

Epifanio, C. C., and D. R. Durran, 2002a: Lee-vortex formation in free-slip stratified flow over ridges. Part I: Comparison of weakly nonlinear inviscid theory and fully nonlinear viscous simulations. *J. Atmos. Sci.,* **59,** 1153–1165, doi:10.1175/1520-0469(2002)059<1153:LVFIFS>2.0.CO;2.

——, and ——, 2002b: Lee-vortex formation in free-slip stratified flow over ridges. Part II: Mechanisms of vorticity and PV formation in nonlinear viscous wakes. *J. Atmos. Sci.,* **59,** 1166–1181, doi:10.1175/1520-0469(2002)059<1166:LVFIFS>2.0.CO;2.

——, and R. Rotunno, 2005: The dynamics of orographic wake formation in flows with upstream blocking. *J. Atmos. Sci.,* **62,** 3127–3150, doi:10.1175/JAS3523.1.

Etling, D., 1989: On atmospheric vortex streets in the wake of large islands. *Meteor. Atmos. Phys.,* **41,** 157–164, doi:10.1007/BF01043134.

Haack, T., S. D. Burk, C. Dorman, and D. Rogers, 2001: Supercritical flow interaction within the Cape Blanco–Cape Mendocino orographic complex. *Mon. Wea. Rev.,* **129,** 688–708, doi:10.1175/1520-0493(2001)129<0688:SFIWTC>2.0.CO;2.

Hanna, S. R., D. G. Strimaitus, J. S. Scire, G. E. Moore, and R. C. Kessler, 1991: Overview of results of analysis of data from the South-Central Coast Cooperative Aerometric Monitoring Program (SCCCAMP 1985). *J. Appl. Meteor.,* **30,** 511–533, doi:10.1175/1520-0450(1991)030<0511:OOROAO>2.0.CO;2.

Heinze, R., S. Raasch, and D. Etling, 2012: The structure of Kármán vortex streets in the atmospheric boundary layer derived from large eddy simulation. *Meteor. Z.,* **21,** 221–237, doi:10.1127/0941-2948/2012/0313.

Hubert, L. F., and A. F. Krueger, 1962: Satellite pictures of mesoscale eddies. *Mon. Wea. Rev.,* **90,** 457–463, doi:10.1175/1520-0493(1962)090<0457:SPOME>2.0.CO;2.

Jiang, Q., and R. B. Smith, 2000: V-waves, bow shocks, and wakes in supercritical hydrostatic flow. *J. Fluid Mech.,* **406,** 27–53, doi:10.1017/S0022112099007636.

Kessler, R. C., and S. G. Douglas, 1991: Numerical simulation of topographically forced mesoscale variability in a well-mixed marine layer. *J. Appl. Meteor.,* **30,** 633–651, doi:10.1175/1520-0450(1991)030<0633:ANSOME>2.0.CO;2.

Lester, P. F., 1985: Studies of the marine inversion over the San Francisco Bay area. . .A summary of the work of Albert Miller, 1961–1978. *Bull. Amer. Meteor. Soc.,* **66,** 1396–1402, doi:10.1175/1520-0477(1985)066<1396:SOTMIO>2.0.CO;2.

Li, X., P. Clemente-Colon, W. G. Pichel, and P. W. Vachon, 2000: Atmospheric vortex streets on a RADARSAT SAR image. *Geophys. Res. Lett.,* **27,** 1655–1658, doi:10.1029/1999GL011212.

Lyons, W. A., and T. Fujita, 1968: Mesoscale motions in oceanic stratus as revealed by satellite data. *Mon. Wea. Rev.,* **96,** 304–314, doi:10.1175/1520-0493(1968)096<0304:MMIOSA>2.0.CO;2.

Mass, C. F., and M. D. Albright, 1989: Origin of the Catalina eddy. *Mon. Wea. Rev.,* **117,** 2406–2436, doi:10.1175/1520-0493(1989)117<2406:OOTCE>2.0.CO;2.

Mosher, F. R., 2013: Attempting to turn night into day; development of visible like nighttime satellite images. *16th Conf. on Aviation, Range, and Aerospace Meteorology,* Austin, TX, Amer. Meteor. Soc., 5.6. [Available online at https://ams.confex.com/ams/93Annual/webprogram/Paper210902.html.]

NCAR, 2014: NCAR Command Language, version 6.2.0. UCAR/NCAR/CISL/VETS, doi:10.5065/D6WD3XH5.

Orlanski, I., 1975: A rational subdivision of scales for atmospheric processes. *Bull. Amer. Meteor. Soc.,* **56,** 527–530.

Parish, T. R., D. A. Rahn, and D. Leon, 2013: Airborne observations of a Catalina eddy. *Mon. Wea. Rev.,* **141,** 3300–3313, doi:10.1175/MWR-D-13-00029.1.

Porter, J. N., D. Stevens, K. Roe, S. Kono, D. Kress, and E. Lau, 2007: Wind environment in the lee of Kauai Island, Hawaii during trade wind conditions: Weather setting for the Helios mishap. *Bound.-Layer Meteor.,* **123,** 463–480, doi:10.1007/s10546-007-9155-z.

Rahn, D. A., T. R. Parish, and D. Leon, 2013: Airborne measurements of coastal jet transition around Point Conception, California. *Mon. Wea. Rev.,* **141,** 3827–3839, doi:10.1175/MWR-D-13-00030.1.

Rosenthal, J., 1968: A Catalina eddy. *Mon. Wea. Rev.,* **96,** 742–743, doi:10.1175/1520-0493(1968)096<0742:ACE>2.0.CO;2.

Ruscher, P. H., and J. W. Deardorff, 1982: A numerical simulation of an atmospheric vortex street. *Tellus,* **34A,** 555–566, doi:10.1111/j.2153-3490.1982.tb01844.x.

Schär, C., and R. B. Smith, 1993: Shallow-water flow past isolated topography. Part I: Vorticity production and wake formation. *J. Atmos. Sci.,* **50,** 1373–1400, doi:10.1175/1520-0469(1993)050<1373:SWFPIT>2.0.CO;2.

——, and D. R. Durran, 1997: Vortex formation and vortex shedding in continuously stratified flows past isolated topography. *J. Atmos. Sci.,* **54,** 534–554, doi:10.1175/1520-0469(1997)054<0534:VFAVSI>2.0.CO;2.

Smolarkiewicz, P. K., and R. Rotunno, 1989a: Low Froude number flow past three-dimensional obstacles. Part I: Baroclinically generated lee vortices. *J. Atmos. Sci.,* **46,** 1154–1164, doi:10.1175/1520-0469(1989)046<1154:LFNFPT>2.0.CO;2.

——, and ——, 1989b: Reply. *J. Atmos. Sci.,* **46,** 3614–3617, doi:10.1175/1520-0469(1989)046<3614:R>2.0.CO;2.

Sun, W.-Y., and J.-D. Chern, 1994: Numerical experiments of vortices in the wakes of large idealized mountains. *J. Atmos. Sci.,* **51,** 191–209, doi:10.1175/1520-0469(1994)051<0191:NEOVIT>2.0.CO;2.

Thompson, W. T., S. D. Burk, and J. Rosenthal, 1997: An investigation of the Catalina eddy. *Mon. Wea. Rev.,* **125,** 1135–1146, doi:10.1175/1520-0493(1997)125<1135:AIOTCE>2.0.CO;2.

Thomson, R. E., J. F. R. Gower, and N. W. Bowker, 1977: Vortex streets in the wake of the Aleutian Islands. *Mon. Wea. Rev.,* **105,** 873–884, doi:10.1175/1520-0493(1977)105<0873:VSITWO>2.0.CO;2.

Thuillier, R. H., 1987: Real-time analysis of local wind patterns for application to nuclear-emergency response. *Bull. Amer. Meteor. Soc.,* **68,** 1111–1115, doi:10.1175/1520-0477(1987)068<1111:RTAOLW>2.0.CO;2.

Wakimoto, R. M., 1987: The Catalina eddy and its effect on pollution over southern California. *Mon. Wea. Rev.,* **115,** 837–855, doi:10.1175/1520-0493(1987)115<0837:TCEAIE>2.0.CO;2.

Wilczak, J. M., W. F. Dabberdt, and R. A. Kropfli, 1991: Observations and numerical-model simulations of the atmospheric boundary layer in the Santa Barbara coastal region. *J. Appl. Meteor.,* **30,** 652–673, doi:10.1175/1520-0450(1991)030<0652:OANMSO>2.0.CO;2.

Young, G. S., and J. Zawislak, 2006: An observational study of vortex spacing in island wake vortex streets. *Mon. Wea. Rev.,* **134,** 2285–2294, doi:10.1175/MWR3186.1.